0Enhancement of Linear Induction Motor Performance Using Indirect Field–Oriented Voltage Control

Dr. Adil Hameed Ahmed
Electrical and Electronic Engineering Department, University of Technology /Baghdad
Emial: dradilh152@yahoo.com.
Hydier yosife Abd
Electrical and Electronic Engineering Department, University of Technology /Baghdad
Emial: hydier_eee@yahoo.com

Received on: 17/4/2012 & Accepted on: 31/1/2013

ABSTRACT

In this work, the mathematical model of linear induction motor (LIM) has been described and the dynamic behaviors have been simulated taking into account the end effects. Firstly, the validity of the LIM model is verified by considering its open loop characteristics; where both no-load and load changed are included. Secondly, a scalar control has been suggested and its robustness against variation of parameters is examined. Finally, the vector control with indirect field oriented control has been included and its simulated results are compared to those of scalar control to show the effectiveness of both control schemes on the robustness measure of LIM behavior. The sophistication and complexity of speed controller is beyond the scope of the work, therefore, a conventional controller based on Proportional Integral (PI) action is sufficient for the present work. The LIM responses such as thrust force, velocity, currents and voltages are simulated and outputted using MATLAB/SIMULINK package (R2010a).

Keywords: Linear Induction Motor, Indirect Field Oriented Control, Scalar Control.

تحسين أداء المحرك الحثي الخطيِّ باستخدام تقنيات المجال الموجه غير المباشر لمسيطر الفولتية

الخلاصـــة:

تم في هذا البحث استنتاج نموذج رياضي للتصرف الديناميكي للمحرك ألحثي الخطي آخذين بنظر الاعتبار التأثيرات المغناطيسية للنهايات الطرفية للمحرك ألحثي الخطي. تم في الجزء الأول استعراض نتائج المحاكاة للنموذج المقترح للمصادقة على صحة عمله في حالات اللاحمل والحمل المفاجئ و تمثيل النموذج المقترح للمحرك ألحثي الخطي باستخدام ال (MATLAB)عن طريق تطبيق ظروف تحميل متعددة تم من خلالها إيجاد استجابة كل من القوة والسرعة والتيار والفولتية. إما الجزء الثاني من البحث فيتعامل مع نظام التحكم ألاتجاهي للمحرك ألحثي الخطي باستخدام طريقة

https://doi.org/10.30684/etj.31.12A.13
2412-0758/University of Technology-Iraq, Baghdad, Iraq

التوجيه غير المباشر للمجال (IFOC), ونتائج التمثيل حسبت أيضا لإظهار صلاحية هذا النظام, ومقارنتها مع نظام التحكم العددي (Scalar Control), كما تم احتساب تأثير المعاملات في نظام السيطرة المقترح. أثبتت نتائج نظام السيطرة أستراتيجية توجيه المجال وأظهار تحسين أداء النموذج المقترح في هذا البحث من خلال مجموعة النتائج التي تم الحصول عليها.

INTRODUCTION

Linear Induction Motors (LIM) are widely used in many industrial applications including transportation, conveyor systems, actuators, material handling, pumping of liquid metal, and sliding door closers.

The most obvious advantage of linear motor is that it has no gears and requires no mechanical rotary-to-linear converters. The driving principles of the LIM are similar to a traditional Rotary Induction Motor (RIM), but its control characteristics are more complicated than the RIM.

The linear induction machines can be obtained (imaginary process) by "*cutting*" a cylindrical induction motor along its radius from the center axis of the shaft to the external surface of the stator core and "*rolling*" it out flat as shown in Figure (1) [1].

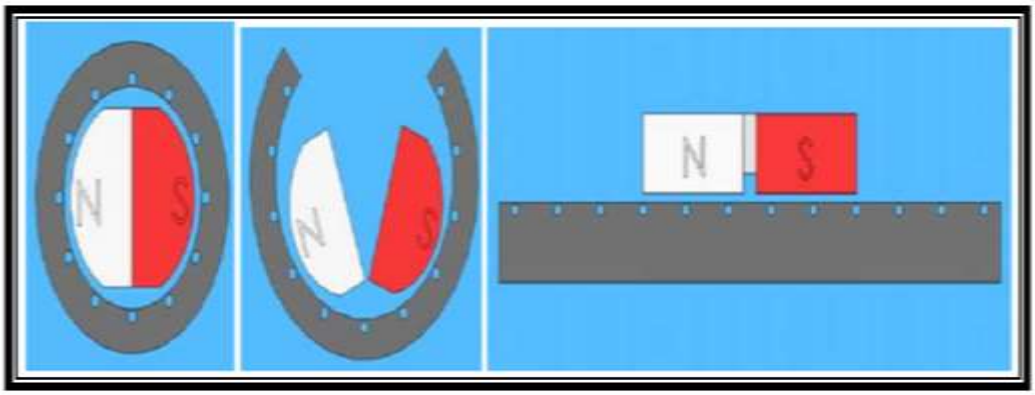

Figure (1) Illustrating the Imaginary process of Unrolling a rotary Motor [1].

In order to obtain high performance of linear motor, it is important to develop vector control for LIM. The basic idea behind the field oriented control is uncoupling the flux and the torque of an induction motor in order to achieve the torque response similar to that of a separately excited direct current machine. The linear induction motor is similar to rotary motor motor except the torque has been replaced by thrust force (propulsion force) and the rotational speed by linear speed. Thus, the field oriented control, can be adopted to decouple the dynamics of the thrust force and the rotor flux amplitude of the LIM [2].

In Linear Induction Motor the flat stator would produce a magnetic field that moves at constant speed. The linear synchronous speed is given by $v_s = 2\tau_p f$; where v_s is the linear synchronous speed (*m/s*), τ_p long of one pole pitch (*m*) and f frequency [*Hz*].

Previous studies clearly indicate that linear synchronous speed does not depend on the number of poles, but depend on the pole pitch Fig.(2). To increase the linear synchronous speed of the LIM, the designer could either [1]:

a. Design a longer pole pitch.

b. Increase the supply frequency.

As it is known, there should be a relative motion between the conductor and the magnetic lines of flux in order for a voltage to be induced in the conductor; that is why induction motors normally operate at a speed v_r that is slightly less than the synchronous velocity v_s.

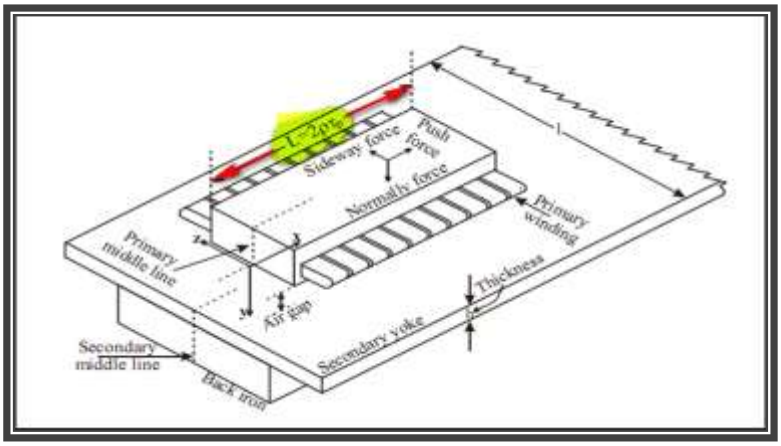

Figure (2): Geometry of single-sided linear induction motor.

The slip formula of the LIM is identical to the conventional rotary induction machine and it is defined as the difference between the stator magnetic field speed and the rotor speed. Slip is the relative motion needed in the linear induction motor to induce a voltage in the rotor (secondary). The per-unit of slip can be given by; $S = (v_s - v_r)/v_s$, where S is the slip v_r is the LIM velocity and v_s is the synchronous velocity of magnetic field [3].

DYNAMIC MODEL OF (LIM) INCLUDING THE END EFFECTS

In order to understand and analyze indirect field oriented control of linear induction motors, the dynamic model is necessary. The dynamic model of the linear induction motor (LIM) can be analyzed by using the *d*-*q* model of the equivalent electrical circuit with end effects included. The *q*-axis equivalent circuit of the LIM is identical to the *q*-axis equivalent circuit of the rotating induction motor (RIM); where its parameters do not vary with the end effects [4]. However, in the d-axis equivalent circuit entry secondary currents affect the air gap flux. When the primary moves, the secondary is continuously replaced by a new material.

It is clear that flux density distribution distortion increase with increasing speed. Therefore, the *d*-axis equivalent circuit of the RIM cannot be used in the LIM analysis when the end effects are considered [5].

The linear induction motor's equivalent *d-q* circuit is different from that of RIM. The LIM's equivalent electrical circuit is shown in Figures (3) and (4). The secondary entry current on the *q*-axis maintains a null reference *q*-axis secondary flux, within a narrow error band. The equivalent *q*-axis electrical circuit for the LIM is identical to that of a conventional induction motor. In this case, the parameters are not changed by the end effects. The gap flux is influenced by the secondary *d*-axis entry currents. Therefore the equivalent *d*-axis electrical circuit associated with a conventional induction motor cannot be used in the analysis of a linear induction motor, if the end effects, as a function of velocity, are to be considered [6].

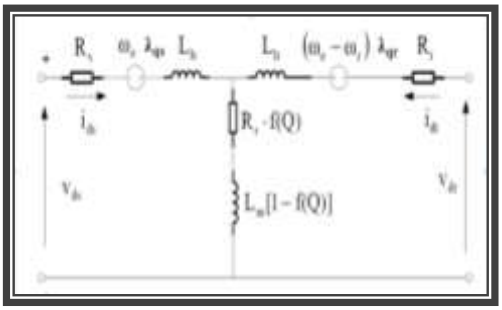

Figure (3) Per-phase equivalent circuit of LIM considering the end effect d-axis equivalent circuit.

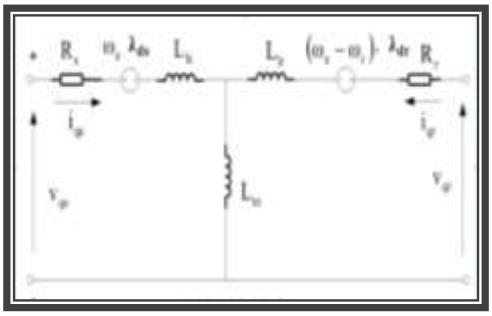

Figure (4) Per-phase equivalent circuit of LIM considering the end effect q-axis equivalent circuit.

Figure (3) and (4) show the d-axis and q-axis equivalent circuits of LIM, respectively. It is clear that magnetization branch in d-axis equivalent circuits is different from the traditional induction motor, while q-axis equivalent circuit is the same as in the traditional induction motor. From the *dq* equivalent circuit of the LIM Figures (3) and (4), the primary and secondary voltage equations in a synchronous reference system (superscript "*e*") aligned with the secondary flux are given by [5]:

$$V_{ds}^{e} = R_s\ i_{ds}^{e} + R_r\, f(Q)(i_{ds}^{e} + i_{dr}^{e}) + \frac{d\lambda_{ds}^{e}}{dt} - \omega_e\, \lambda_{qs}^{e} \quad \text{...(1)}$$

$$V_{qs}^{e} = R_s\, i_{qs}^{e} + \frac{d\lambda_{qs}^{e}}{dt} + \omega_e\, \lambda_{ds}^{e} \quad \text{…(2)}$$

$$V_{dr}^{e} = R_r\ i_{dr}^{e} + R_r\, f(Q)(i_{ds}^{e} + i_{dr}^{e}) + \frac{d\lambda_{dr}^{e}}{dt} - \omega_{sl}\lambda_{qr}^{e} = \quad \text{…(3)}$$

$$V_{qr}^{e} = R_r\, i_{qr}^{e} + \omega_{sl}\, \lambda_{dr}^{e} = 0 \quad \text{…(4)}$$

where (V_{ds}^{e}, V_{qs}^{e}) , (i_{ds}^{e}, i_{qs}^{e}) and $(\lambda_{ds}^{e}, \lambda_{qs}^{e})$ are the *dq*-axis voltages, currents and flux linkages of the primary, respectively, and, (V_{dr}^{e}, V_{qr}^{e}) , (i_{dr}^{e}, i_{qr}^{e}) and $(\lambda_{dr}^{e}, \lambda_{qr}^{e})$ are the *dq*-axis voltages, currents and flux linkages of the secondary, respectively. ω_e denotes the secondary angular speed and ω_{sl} denotes the slip frequency, $f(\mathrm{Q})$ is

factor linked to the primary length (end effects). The subscript *r* and *s* denotes the secondary and stator values respectively referred to the stator, and the subscripts *d* and *q* denote the *dq*-axis components in the arbitrary reference frame. The linkage fluxes are given by the following equations [7,8]:

$$\left.\begin{aligned}\lambda_{ds} &= L_{ls}i_{ds} + L'_m(i_{ds} + i_{dr})\\ \lambda_{qs} &= L_{ls}i_{qs} + L_m(i_{qs} + i_{qr})\\ \lambda_{dr} &= L_{lr}i_{dr} + L'_m(i_{ds} + i_{dr})\\ \lambda_{qr} &= L_{lr}i_{qr} + L_m(i_{qs} + i_{qr})\end{aligned}\right\} \quad \ldots(5)$$

where;
L_{ls} : the primary leakage inductance,
L_{lr}: the secondary leakage inductance,
L_m : the magnetizing inductance,
L'_m: the magnetizing inductance with end effect,
L_s : the primary inductance,
L_r : the secondary inductance,

The magnetizing inductance with end effect is given by;

$$L'_m = L_m(1 - f(Q)) \quad \ldots(6)$$

The primary inductance and the secondary inductance are given, respectively, as

$$L_s = L_{ls} + L_m \quad \ldots(7)$$

$$L_r = L_{lr} + L_m \quad \ldots(8)$$

From the primary and secondary voltage equations in a synchronous reference system, the linkage flux can be obtained from the following differential equations:The linkage fluxes of *ds*- axis:

$$\begin{aligned}&\frac{d\lambda_{ds}}{dt}\\ &= \left[\frac{-R_s L_r - R_r L_r f(Q) + R_s L_m f(Q) + R_r f(Q) L_m}{M}\right]\lambda_{ds}\\ &+ \left[\frac{R_s L_m - R_s L_m f(Q) + R_r L_m f(Q) - R_r L_s f(Q)}{M}\right]\lambda_{dr} + V_{ds}\end{aligned} \quad \ldots(9)$$

where $M = \big(L_s - L_m f(Q)\big)\big(L_r - L_m f(Q)\big) - L_m^2\big(1 - f(Q)\big)^2$

Change of the linkage fluxes with respect to time in *qs*-axis, *dr*-axis and *qr*-axis are given by
the following equations:

$$\frac{d\lambda_{qs}}{dt} = \left[\frac{R_s L_m}{L_\sigma}\right]\lambda_{qr} - \left[\frac{R_s L_r}{L_\sigma}\right]\lambda_{qs} + V_{qs} \quad \ldots(10)$$

$$\frac{d\lambda_{dr}}{dt} = \left[\frac{-R_r L_s - 2R_r L_m f(Q) - R_r L_s f(Q)}{M}\right]\lambda_{dr} + \left[\frac{R_r L_m - R_r L_r f(Q)}{M}\right]\lambda_{ds} + \left[\frac{\pi V_r}{\tau_p}\right]\lambda_{qr} \quad \ldots(11)$$

$$\frac{d\lambda_{qr}}{dt} = \left[\frac{\pi V_r}{\tau_p}\right]\lambda_{qr} - \left[\frac{R_r L_s}{L_\sigma}\right]\lambda_{qr} + \left[\frac{R_r L_m}{L_\sigma}\right]\lambda_{qs} \quad \ldots(12)$$

where ω_{sl} and rotor speed are given, respectively;

$$\omega_{sl} = \omega_e - \omega_r \quad \ldots(13)$$

$$\omega_r = \frac{\pi}{\tau_p} V_r \quad \ldots(14)$$

The electromagnetic thrust (force) can be given as:

$$F = \frac{\pi}{\tau_p} T_{em} \quad \ldots(15)$$

where F_e is the electromagnetic thrust force, τ_p is the pole pitch and T_{em} is the electromagnetic torque which is given by

$$T_{em} = \frac{3}{2}\frac{P}{2}\left(\lambda_{ds} i_{qs} - \lambda_{qs} i_{ds}\right) \quad \ldots(16)$$

where P is the number of pole pairs. Therefore, the thrust force equation becomes

$$F_e = \frac{3\pi}{2\tau_p}\frac{P}{2}\left(\lambda_{ds} i_{qs} - \lambda_{qs} i_{ds}\right) \quad \ldots(17)$$

Substitution of i_{qs}, i_{ds} into Eq. (17) yields;

$$F_e = K_F\left[\lambda_{ds}\left(\frac{L_r\lambda_{qs} - L_m\lambda_{qr}}{L_\sigma}\right) - \lambda_{qs}\left(\frac{\left(L_r - L_m f(Q)\right)\lambda_{ds} - L_m\left(1 - f(Q)\right)\lambda_{dr}}{M}\right)\right] \quad \ldots(18)$$

where K_F is given by

$$K_F = \frac{3\pi}{2\tau_p}\frac{P}{2}$$

Using Eq.s (9)-(12) one can easily develop the state-space model for linear induction motor developed in stationary reference frame with modulus of the linkage flux to index a_{jk} as given below:

$$\begin{bmatrix} \dot{\lambda}_{ds} \\ \dot{\lambda}_{qs} \\ \dot{\lambda}_{dr} \\ \dot{\lambda}_{qr} \end{bmatrix} = \begin{bmatrix} a_{11} & a_{12} & a_{13} & a_{14} \\ a_{21} & a_{22} & a_{23} & a_{24} \\ a_{31} & a_{32} & a_{33} & a_{34} \\ a_{41} & a_{42} & a_{43} & a_{44} \end{bmatrix} \begin{bmatrix} \lambda_{ds} \\ \lambda_{qs} \\ \lambda_{dr} \\ \lambda_{qr} \end{bmatrix} + \begin{bmatrix} 1 & 0 \\ 0 & 1 \\ 0 & 0 \\ 0 & 0 \end{bmatrix} \begin{bmatrix} V_{ds} \\ V_{qs} \end{bmatrix} \quad \dots (19)$$

SIMULATED RESULTS

Simulink has the advantages of being capable of complex dynamic system simulations. The dynamic model of single-side LIM with end effect has been coded in m-file with an s-function structure. Then this file is included in Simulink using s-function block. It is worth to mention that the dq-model of LIM requires that all the three-phase variables have to be transformed to the two-phase synchronously traveling frame.

OPENO-LOOP CHARACTERISTICS OF (LIM)

The block diagram of SLIM simulation based on MATLAB/ SIMULINK is shown in Fig.(5). In this simulation the characteristics of open-loop system has been considered. The inputs of linear induction motor are three-phase voltage, their fundamental frequency, and the load force. On the other hand, the outputs are the three-phase currents, thrust force, and the rotor speed. No feedback has been detected in this simulation and, therefore, it is expected that the change in motor parameters would never be compensated.

It should be emphasized that the dynamic model of LIM including end-effect are coded inside m-file with s-function structure and this m-file is fetched at SIMULINK level by an s-function block. Therefore, at each simulation instant this m-file is executed to yield the machine different responses. Figure (6) and (7) show the speed and thrust variations, respectively, at no-load condition. It is clear from Fig.(6) that the speed reaches rated value within 10 $msec$.

To show the effect of load on motor dynamic behavior, a load of different levels are applied to the motor. The wave-form of the applied load is shown in Figure (8). At the interval of applying load, the dip in motor speed response increases with level value of exerted load. The variations of speed and electromagnetic force with time during load intervals are shown in Figure (9) and Figure (10) respectively for direct source voltages.

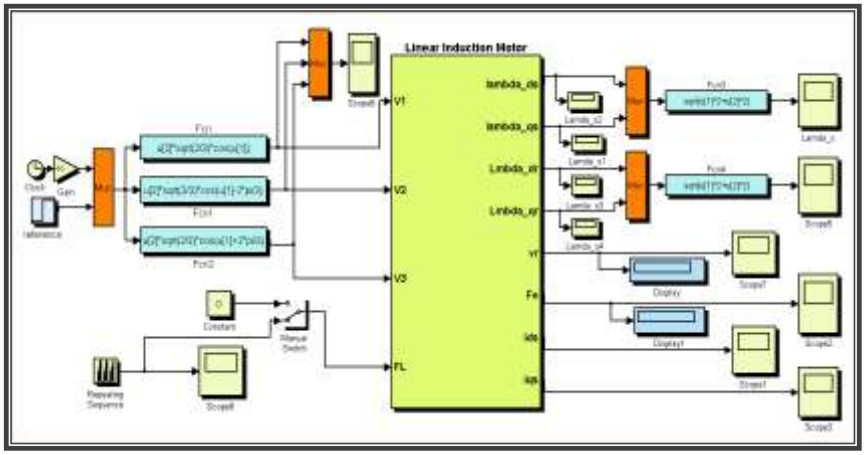

Figure (5) Simulink modeling of LIM using s-function

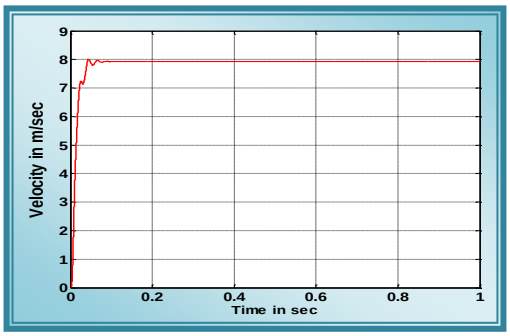

Figure (6) Speed response.

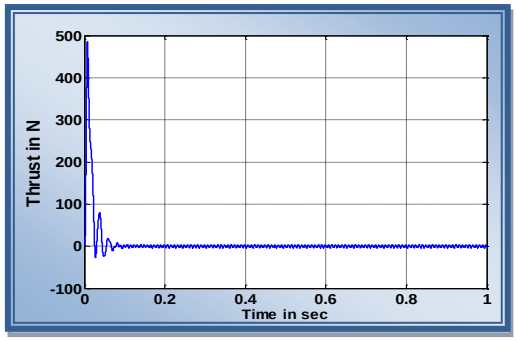

Figure (7) The thrust force response

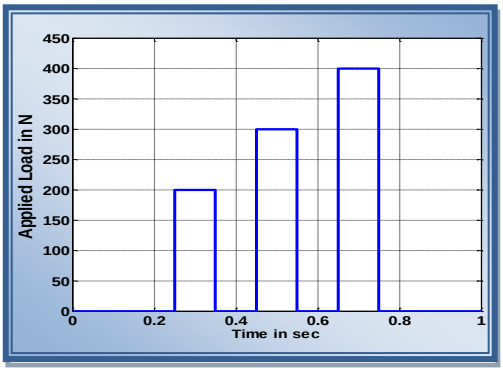

Figure (8) The variation of load exertion

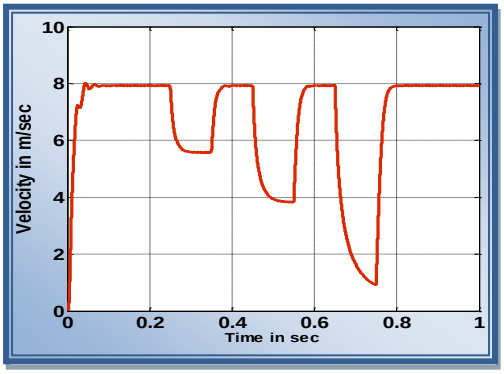

Figure (9) Speed variation of LIM at different Load levels

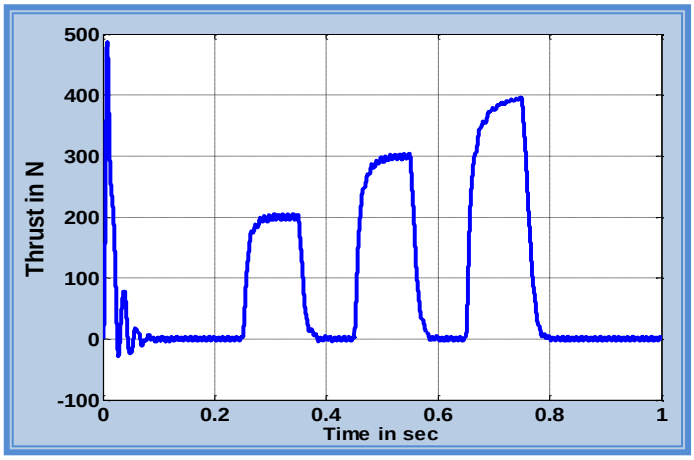

Figure (10) Electromagnetic force (Thrust) variation of LIM at variable load.

MODELING AND SIMULATION OF SCALAR CONTROL SYSTEM

Scalar control, which is called Volt/Hertz control, it regulates the ratio of voltage with frequency at a constant value. The Simulink modeling of scalar-controlled LIM is shown in Fig.(11). The speed controller is confined by a PI controller. Therefore, two terms of PI controller have been tuned; the proportional gain (k_p) and the integral gain (k_i).

The best values of PI controller terms can be found using "Trial and Error" principle. The best gains are those which give the best response. Many simulation tests lead to a final best proportional gain (k_p) to be 10 and integral gain (k_i) of 0.01.

Figure (12) shows the speed response at the same levels of exerted load. As compared to corresponding open-loop case, one can easily notice that the dip in speed response is less than shown in its counterpart in open-loop case. Therefore, the speed behavior show more robustness than that with open-loop case.

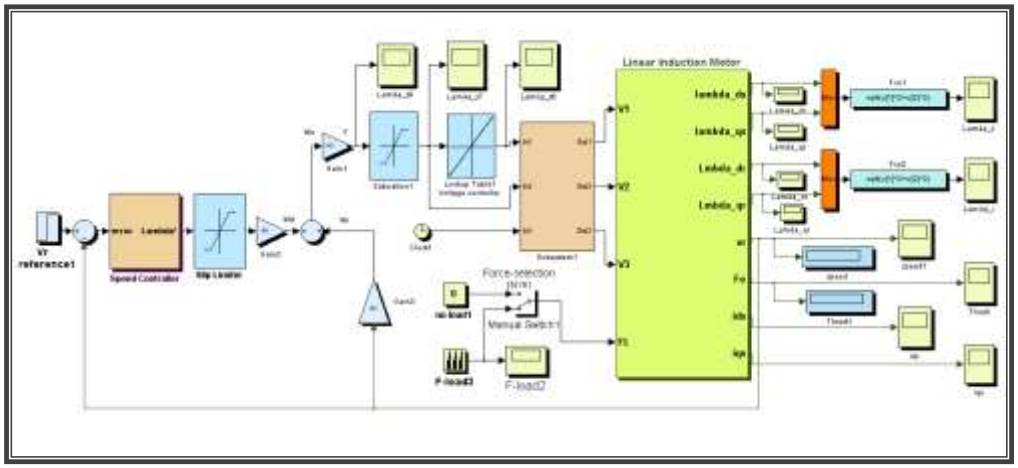

Figure (11) Simulink Model of scalar controlled linear induction motor.

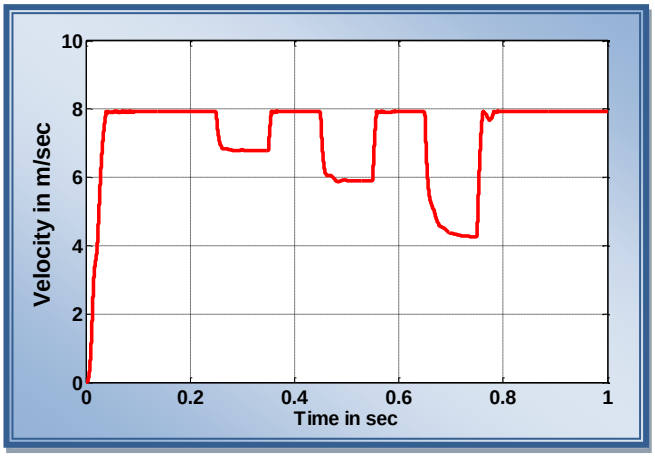

Figure (12) Speed at variable load with scalar controlled.

SIMULATION OF (IFOC) CONTROL SYSTEM

The fundamental intention of this Simulink design, is that the (IFOC) control as shown in Figure (13), portion of the design will cause the secondary generate a speed profile that follows the commanded speed input V_r^*. To do this, the commanded speed signal is fed into the IFOC section, where it is subtracted from the measured speed of the secondary V_r . The error generated is then fed into a thrust controller block. The determination of these two parameters can be tuned by "Trial and Error" principle to get the best controller response. After many testing and running in the simulation, the final best parameters values are Proportional gain (k_p): 30, Integral gain (k_i): 0.001.

The results of indirect field oriented controlled for linear induction motor speed, and electromagnetic force (Thrust) during same applied load variation with time, are shown in Figures (14) and (15) respectively.

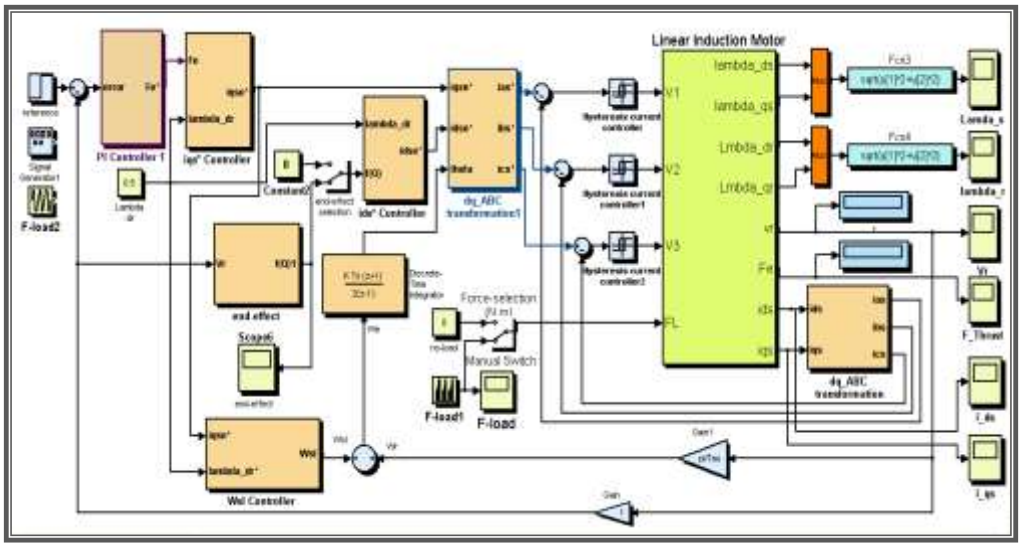

Figure (13) Simulink Model of IFO controlled linear induction motor.

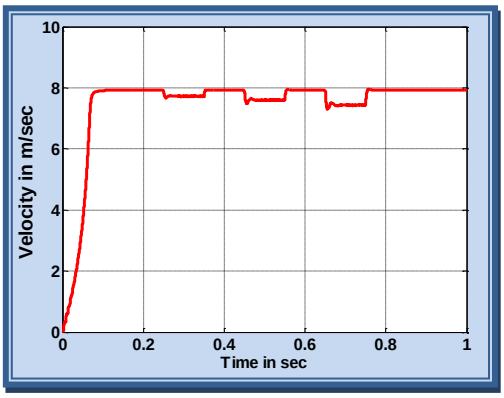

Figure (14) Speed response with variable Load

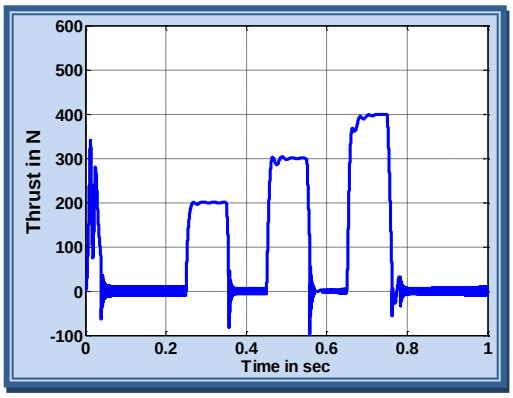

Figure (15) Force (Thrust) response with variable Load

CONCLUSION

Based on observations of simulated results, the following points can be highlighted:

1. Results from open-loop characteristics show that both velocity and thrust responses are monotonic and stable. However, any change in load would lead to large change in motor responses. This is evident in relevant figures. This indicates that the system with open-loop is robust-less and unreliable.
2. Scalar control shows better responses than open-loop case. However, the change of machine response due to load change is still considerable. This of course due to coupling effect which leads to an adverse effect in machine behavior.
3. Including IFOC better enhances the machine behavior. This technique would lead to decoupling model. This will increase efficiency and will lead that any change in machine current would convert directly to the thrust force, which would in turn lead to fast change in speed. The IFOC together with PI controller would improve the dynamic of LIM.
4. Results show that the integral gain is considerably small, i.e., no integration action is required and the control action is mainly dependent on proportional gain.

REFERENCE

[1] Kaoru Iwaki, Toshimitsu Morizane, Noriyuki Kimura and Katsunori Taniguchi, "Characteristics of forces of Linear Induction Motor driven by power source including frequency component synchronous with the motor speed", IEEE, International Conference on Electrical Machines and Systems, DOI: 10.1109/ICEMS, October, 2009.

[2] I. Boldea and S. A. Nasar "The Induction Machine Handbook " CRC press LLC, 2002.

[3] M. N. Bandyopadhyay, " Electrical Machines Theory and Practice", Book, Prentice-Hall, New Delhi, India, 2007.

[4] J. Liu, F. Lin, Z. Yang and Trillion Q. Zheng, "Field Oriented Control of Linear Induction Motor Considering Attraction Force & End-Effects", IEEE, Power Electronics and Motion Control Conference, Vol. 1, June 2006.

[5] Chee-Mun Ong, "Dynamic Simulation of Electric Machinery Using Matlab/Simulink", Prentice Hall PTR, New Jersey, 1998.

[6] E. F. Silva, E. B. Santos, C. M. Machado and A. A. Oliveira "vector control for linear induction motor" IEEE, Industrial Technology International Conference, Vol. 1, 2003.

[7] E. F. Silva and J. W. L. Nerys "Field oriented control of linear induction motor taking into account end-effects " IEEE, Advanced Motion Control, Vol. 4, August, 2004.

[8] J. Liu, X. You and Trillion Q. Zheng, "Sliding-mode Variable Structure Current Controller for Field Oriented Controlled Linear Induction Motor Drive ", IEEE, Power Electronics and Motion Control Conference, 10.1109/IPEMC.2009.5157537, June, 2009.